Discover Geoscience

RESEARCH Open Access

21st century Northern Hemisphere warming in a 2025-year context of climatic events using tree-ring data

Samuli Helama[1*]

*Correspondence:
Samuli Helama
samuli.helama@luke.fi
[1]Natural Resources Institute Finland, Rovaniemi, Finland

Abstract

In this study, previously built community ensemble reconstruction, fully based on tree-ring proxy data, is used as a precisely estimated preindustrial-to-present-day temperature scale for Northern Hemisphere summer (June through August) variability over the past two thousand years, against which the recent variability in the observed record was evaluated. The proxy data verified successfully against temperature variability defined by grid boxes extending the tree-ring sites by plus/minus 10 degrees latitudinally and longitudinally (but not over wider spatial scales) over the 1921–2010 period. Summer 2024 was the warmest in the instrumental record, 2.8 °C above the preindustrial 1850–1900 reconstruction mean. In comparison, the warmest and coldest reconstructed summers in AD 246 and AD 536 were, respectively, 1.5 °C and 5.5 °C colder than the 2024 warmth. This means that the full range of natural climate variability was 4.0 °C, which was increased to 5.5 °C by 21st century warming. Temporal pattern of the warmest and coldest preindustrial 1-year temperature events reflected the long-term climatic swings previously described in paleoclimate literature through the Roman Warm Period, AD 536/540s event, Mediaeval Warm Period and Little Ice Age. Despite the improvements in the data processing, the reconstruction still contains considerable uncertainties. A future aim should be to develop denser tree-ring networks to fully cover the extra-tropical Northern Hemisphere land temperature grid boxes for an improved evaluation of the preindustrial and 21st century climatic events, for which purpose the Roman Warm Period appears an interesting, yet largely unexplored, climatic feature.

1 Introduction

The surface of our planet has warmed markedly over the past years and decades. The primary evidence for this change is formed by instrumental air and sea surface temperature records [1–7]. Among these records, land surface air temperature data show global scale warming by 1.7 °C from 1861 to 1900 by the end of the 2010s [8]. Similarly, temperature trends for the periods 1979–2019, 1951–2019, 1900–2019 and 1850–2019 were estimated to be 0.296, 0.219, 0.119 and 0.081 °C per decade, respectively [9]. More recently, the global temperature series show 2023 as the warmest year on record [10], while even

slightly warmer sea surface temperatures were recorded in 2024 [11]. Moreover, regional data indicate that summer 2025 was the hottest on record at least in some parts of the Northern Hemisphere [12]. These estimates among others portray highest temperatures in recent years and trends that have become more progressive over the recent past, with increased warming rate after 1990 [13]. The results are of particular importance in the context of the 2015 Paris Agreement that pursues efforts to limit global warming to 1.5 °C from preindustrial temperature levels [14].

Although the longest gridded land temperature records are available since 1753 [5], similarity among the temperature records created by different research groups increases from 1873, that is, after the guidelines for instrumental observations were internationally standardised [15]. In fact, the instrumental temperatures are typically reported on global and hemispheric scales since 1850, before which date temperature estimates are commonly based on proxy (indirect) records sensitive to climatic variations. The proxy data comprise physical, chemical and biological archives such as ice cores, sediments, speleothems, pollen and other microfossils, plant and other macrofossils, tree rings, corals and other calcareous organisms [16]. These non-instrumental observations can be transformed into the scale of instrumental data and presented in the form of quantitative paleoclimate reconstructions and as such compared with the estimates of recent climatic events, essentially those arisen from the 20th and 21st century temperature trends.

Recent proxy studies have focussed on high-resolution late Holocene records. As an example, geochemical paleothermometer from sclerosponge carbonate skeletons showed nearly constant preindustrial ocean temperatures from 1700 until the early 1860s, increase in temperatures until the late 20th century, and global warming 1.7 ± 0.1 °C above pre-industrial levels by 2020 [17]. A tree-ring based approach placed the 21st century Northern Hemisphere warming in the context of a 2000-year temperature history to provide the current warming a long-term preindustrial context [18]. While the originally published results showed 2023 summer temperatures exceeding the 95% confidence range of natural climate variability by more than 0.5 °C, re-evaluation of the analyses [19] led to a corrigendum suggesting that summer of 2023 exceeded this range of natural climate variability by 0.39 °C. The results were obtained by a comparison between the observed (2023) and reconstructed (AD 246) June-August temperatures. Later, Rantanen et al. [20] used a similar tree-ring approach to show that summer 2024 was very likely the warmest in 2000 years in northern Fennoscandia.

The main aim of this study is to employ a previously compiled community ensemble reconstruction (CER) [21] for demonstrating annually resolved proxy-based Northern Hemisphere summer (June through August) temperature variability over the past two thousand years, for placing the 21st century warm events on precisely estimated temperature scale of this era, and showcasing the importance of rigorous calibration/verification process the reconstruction must undergo prior to any paleoclimatic interpretations. A previous analysis of the same tree-ring dataset [18] terminated for the summer of 2023, for which the current study provides an update. Another reason for the present study stems from the fact that the transformation of CER data was previously carried out over the 1901–2010 period, excluding the 19th century part of the instrumental temperature record [5] as faulty, suggestively due to a lack of station records in remote regions and an exposure bias in early temperature observations [18]. However, it has been shown that at least the exposure bias has likely affected the instrumental

Table 1 Characterization of tree-ring proxy data

N	Tree species	Latitude	Longitude	Last year
1	PIUAL	37–41° N	114–120° W	2009
2	PIUAI	35° N	111° W	2002
3	PCMA	53–54° N	70–72° W	2016
4	PIEAB, LAXDE	46–47° N	11–13° E	2016
5	PIUSI	67–69° N	18–21° E	2010
6	LAXSI	67–70° N	69–72° E	2015
7	LAXGM	71–73° N	85–95° E	2011
8	LAXSI	49–50° N	85–90° E	2017
9	LAXKA	66–71° N	110–150° E	2016

Tree-ring records from nine sites around northern hemisphere are described by running number (N; from west to east), tree species referred to by their EPPO codes (EPPO code system, http://eppt.eppo.org/), latitude, longitude, and the most recent calendar year (Last year). See Ref [21]. for more detail information

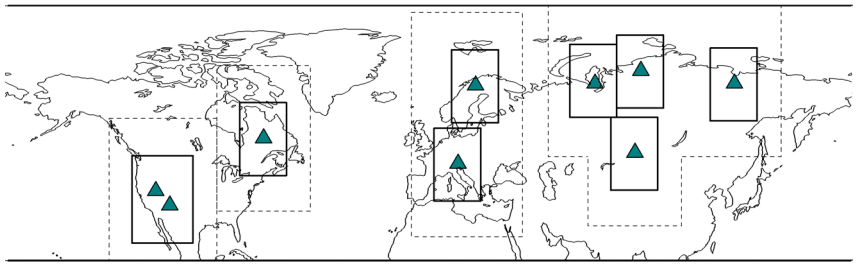

Fig. 1 Tree-ring sites (triangles) from the extra-tropical Northern Hemisphere constituting the community ensemble reconstruction. Regions with continuous and dashed contours refer to grid boxes around the sites plus/minus 10 and 20 degrees latitudinally and longitudinally

observations not only during the 19th century but also in the first 20th-century decades [21–23]. This hypothesis that so far remains unexplored for this tree-ring dataset is analysed in the present paper. On these grounds, it is hypothesised that the inclusion of temperature data from the early 20th-century decades may deflate the proxy-based temperature reconstructions and therefore critically impair the comparisons of preindustrial and instrumental temperature estimates.

1.1 Climatic data

Dataset of community ensemble reconstruction (CER) [21] is formed by tree-ring records from nine sites around the Northern Hemisphere. All these records cover the past two thousand years i.e. Anno Domini/Common Era. Taxonomically, the data represent pine (*Pinus longaeva*, *P. artistata*, *P. sylvestris* and *P. cembra*), spruce (*Picea mariana*) and larch (*Larix decidua*, *L. sibirica*, *L. gmelinii* and *L. cajanderi*) species (Table 1). The data originate from three sites in North America, two sites in Europe, and three sites in northern Siberia, one of them representing inner Eurasia (Fig. 1). These Northern Hemispheric sites represent high-latitude and altitude conditions where tree growth remains sensitive to summer temperature [24–26]. Importantly, this relationship is a prerequisite to reconstruct temperature histories from annual values of tree-ring chronologies. This dataset of 10,437 tree-ring width series were previously analysed by fifteen expert groups of dendrochronologists, working independently, with a goal to produce large-scale Northern Hemisphere temperature reconstruction. Their work included site and series selection, correction for biological age trends in raw tree-ring width data, and the climate calibration procedure to transform the proxy data into temperature

estimates. These data and analyses have been detailed in a previous paper [21]. That study also calculated the mean of the fifteen individual ensemble members to produce the Common Era temperature reconstruction, which is the timeseries (AD 1-2010) examined in this study.

The Berkeley Earth June-August (JJA) instrumental land temperature record was used for comparisons with CER data. The Berkeley Earth dataset [5] is based on a mathematical framework to produce large-scale averages of temperature changes from instrumentally observed data. Temperature values are interpolated to the selected locations on the Earth using the statistical method known as Kriging, which allows inclusion of short and discontinuous temperature records to increase the amount of available data. This dataset was used since the gridded temperature product was available until the summer 2025 when the analyses were run. Moreover, the use of this temperature product made new results fully comparable with earlier studies using the same set of instrumental and proxy data [18, 21]. That is, the Berkeley Earth land temperature record 30–90° was recently employed as a target data for a JJA temperature reconstruction [18]. First, the same instrumental timeseries was adopted for comparisons with CER and referred to hereafter as NH-JJA. Second, regionally more limited records of Northern Hemisphere temperatures were calculated as (i) the mean of the nine sampling sites, referred to hereafter as NHS-JJA, (ii) the mean of land temperature grid boxes, each of the boxes extending the sampling sites plus/minus 10 degrees latitudinally and longitudinally (NH10-JJA), and as (iii) the mean of land temperature grid boxes, each of the boxes extending the sampling sites plus/minus 20 degrees latitudinally and longitudinally (NH20-JJA). In practice, the number of boxes was reduced to eight, due to proximity of the two westernmost sites (see Fig. 1). The spatially more limited temperature estimates were produced and compared with CER data due to the fact that tree growth is primarily controlled by their local climate conditions, rather than those recorded on hemispheric scales. While the climate around the CER sites may reflect the large-scale temperature variability to some extent, the correlations of trends and other temperature patterns are possibly decreasing over such extended spatial scales. In this study, this effect was evaluated by comparing CER data with instrumental temperature records of varying spatial scales, ranging from local to hemispheric (see below).

1.2 New temperature reconstructions

CER data were calibrated to Berkeley Earth land temperature record. To do so, the mean and variance of CER data were adjusted (scaled) to equal that of the instrumental record. To prove the validity of the results, the reconstructed temperature estimates need to be compared with instrumental temperature values withheld from calibration. The validation was carried out using cross calibration/verification exercise [27]. The instrumental period under investigation was divided into early calibration/late verification and late calibration/early verification subperiods. Coefficient of determination (R^2) was used as the calibration statistic and the squared coefficient of (Pearson) correlation (r^2), reduction of error (RE) and coefficient of efficiency (CE) as verification statistics. RE and CE statistics have been presented by Fritts [28] and Briffa et al. [29] and have since then been routinely used in dendroclimatic studies where climate variability is being reconstructed from tree-ring proxy data. The RE and CE are determined as

$$RE = 1.0 - \frac{\sum_{i=1}^{n}(x_i - \widehat{x}_i)^2}{\sum_{i=1}^{n}(x_i - \bar{x}_c)^2}$$

$$CE = 1.0 - \frac{\sum_{i=1}^{n}(x_i - \widehat{x}_i)^2}{\sum_{i=1}^{n}(x_i - \bar{x}_v)^2}$$

where n is the number of years over the verification period, x_i and $\hat{x}_i$ are the instrumental and reconstructed temperature in year i, and the $\bar{x}_c$ and $\bar{x}_v$are the means of instrumental temperature data over the calibration and verification period, respectively. In comparison, CE is more rigorous than RE, for which reason CE obtains lower values than RE, except when the instrumental data have identical means over the calibration and verification periods, in which case RE are CE will result in identical scores. Minimum standards for valid verification statistics are RE > 0 and CE > 0 [28, 29].

In this study, the calibration and verification statistics were at first calculated over the 1901–1955 and 1956–2010 subperiods. To do so, CER data were first calibrated using NH-JJA record over the early (1901–1955) subperiod, and the data withheld from calibration were used to verify the reconstruction skill over the late (1956–2010) subperiod. Second, the cross calibration/verification exercise [27] was continued by calibrating the CER data using the same instrumental temperature record over the late (1956–2010) subperiod and verifying the resulting temperature estimates against the instrumental values over the early (1901–1955) subperiod.

Previously, the earliest part of the instrumental record (1850–1900) was left out from the calibration due to problems arising when comparing the instrumental and CER records of the same interval, these problems being linked with the exposure bias of early temperature observations [18]. Indeed, the exposure bias of instrumental observations has been acknowledged since the mid-19th century [30]. However, the year 1900 may actually be a too early date for the avoidance of the problem, as shown by available evidence from independent estimations suggesting the bias has likely affected instrumental observations until the first 20th-century decades [22, 23]. For this reason, the calibration (R^2) and verification statistics (r^2, RE and CE) were also calculated using the 1921–1965 and 1966–2010 subperiods as the early and late subperiods, these calculations representing a second set of the calibration/verification exercise. The algorithms tailored [31] to execute the procedures elaborated by Ebisuzaki [32], to estimate p values for R^2 and r^2, were exploited.

Third, in seek for an appropriate statistical model, CER data were also calibrated and verified against instrumental data representing the temperature conditions around the tree-ring sites. For this purpose, the calibration and verification statistics were also calculated using NHS-JJA, NH10-JJA and NH20-JA records.

1.3 Temperature uncertainty range

Confidence interval around the reconstructed temperature was determined by a bootstrapping technique, following previous research efforts for tree-ring data [33]. The upper and lower bounds of the 95% range were quantified for the temperature reconstructions using bootstrapping with 10,000 replicates. The individual ensemble members comprising CER data were randomly sampled (with replacement) to estimate annual

means mimicking the replication of the original CER data that vary between nine and fifteen between 1 and 2010 CE.

The mean and variance of the surrogate records ($n = 10{,}000$) produced by bootstrapping were each adjusted to equal that of instrumental data. The upper and lower bounds of the 95% range were adopted as the 2.5th and 97.5th percentiles of the surrogate records. Subsequently, the reliability of the surrogate records, from which the upper and lower bounds of the 95% range were computed, was evaluated, using the methods detailed above. The calibration (R^2) and verification statistics (r^2, RE and CE) were calculated over the subperiods.

2 Results

2.1 Calibration and verification

Scaling CER to NH-JJA temperature data indicated no reconstruction skill over the early subperiod (1901–1955). Over this interval, both RE and CE statistics resulted in strongly negative outcomes (Fig. 2a). These outcomes result from an offset between NH-JJA and CER records over the early 20th century, i.e. between the instrumental and proxy evidence, until ~1920 (Fig. 2e). Further investigation of the issue showed that CER data did not verify successfully against NH-JJA temperatures even when the pre-1920s data were left out from the calibration/verification exercise. That is, the reconstruction still displayed negative verification outcomes over the 1921–1965 subperiod (Fig. 2e). These outcomes suggest that CER data may not be fully representative of the large-scale temperature variations represented by NH-JJA record (i.e. north of 30°N).

Further exploration of the spatial representativeness suggests that CER data may indeed better correspond to temperature variability around the tree-ring sites

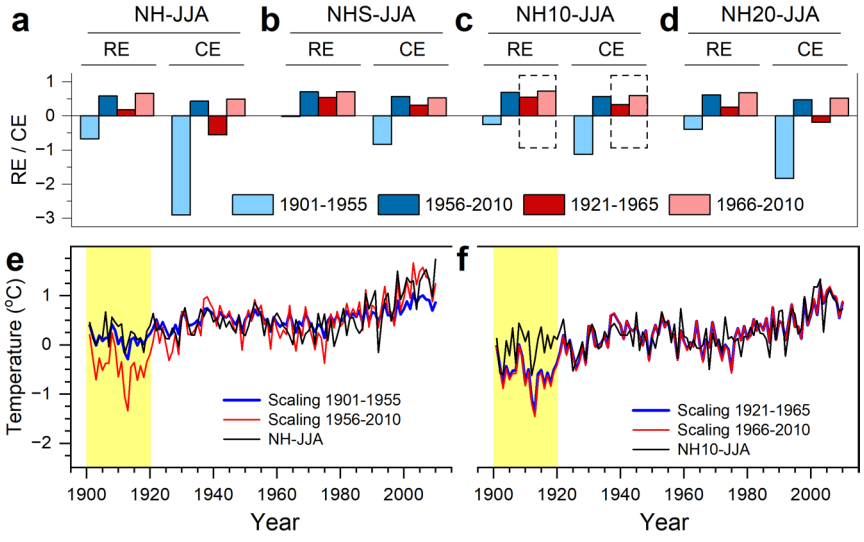

Fig. 2 Verification of reconstructions. Verification statistics resulting from scaling CER against the instrumental land temperature records (June through August; JJA) for temperatures averaged over the 30–90°N region (NH-JJA) (**a**), temperatures averaged over the tree-ring sites (NHS-JJA) (see Table 1 for coordinates) (**b**), and over the grid boxes around the sites plus/minus 10 degrees (NH10-JJA) (**c**) and 20 degrees (NH20-JJA) latitudinally and longitudinally (**d**). The Reduction of Error (RE) and Coefficient of Efficiency (CE) statistics were calculated for early period from scaling over late period, and vice versa. For NH10-JJA, the boxes with dashed contours indicate positive RE and CE outcomes for scaling against the mean JJA instrumental land temperature record of NH10 areas used as target variable building the temperature reconstruction of this study (**c**). CER scaled against NH-JJA (**e**) and NH10-JJA data (**f**), separately over the early and late halves of the instrumental periods as discussed in the text. The 1901–1920 period discussed in the text is highlighted with yellow shading

(Fig. 2b–d). When the early 20th century is left out from calibration/verification trials, CER data showed positive verification statistics (1921–2010) when scaled against NHS-JJA (Fig. 2b) or NH10-JJA records (Fig. 2c), but not over larger areas (NH20-JJA) (Fig. 2d). That scaling CER data to temperature grid boxes wider than plus/minus 10 degrees around the tree-ring sites did not show invariably positive verification outcomes is logical since the extended area is reaching spatial scales of NH-JJA data (see Fig. 1). Indeed, Pearson correlation between NH-JJA and NH20-JJA was $r = 0.97$ over this period (1921–2010), whereas NH-JJA and NH10-JJA correlated with $r = 0.88$.

Guided by the positive verification statistics, new temperature reconstruction was obtained by scaling CER data to instrumental NH10-JJA (1921–2010) temperatures. The calibration and verification statistics of the reconstruction are detailed in Table 2. Hereafter, the NH10-JJA reconstruction was used to provide the current warming a preindustrial context of past climate variability.

Additional details on the reconstruction skill were obtained by bootstrapped CER data ($n = 10{,}000$) showing R^2 and r^2 between 0.72 and 0.25 against NH10-JJA record (Fig. 3a, b). Moreover, late verification (1966–2010) showed RE to vary between 0.74 and 0.41 and CE between 0.70 and 0.32 (Fig. 3c, d), whereas RE from early verification (1921–1965) ranged from 0.78 to 0.58 and CE from 0.47 to 0.01 (Fig. 3e, f). All these outcomes fulfil the RE > 0 and CE > 0 criteria, which further reinforces the credibility of the new reconstruction.

2.2 New temperature reconstruction

Highest summer temperatures were observed during the 21st century, the summers 2023 and 2024 being the two warmest on record (Figs. 4 and 5a). Temperatures 2 °C above the preindustrial 1850–1900 reconstruction mean have been recorded since 2012, after which date similarly high temperatures had occurred ten times. Moreover, the same level has been exceeded continuously every year since 2018. In the context of the two-thousand-year-long proxy-based reconstruction, ten warmest summers had all occurred since 1994, over which years the temperatures have remained 1.5 °C above the preindustrial 1850–1900 reconstruction mean (Table 3a). In comparison, the warmest preindustrial summer was recorded in AD 246 with temperature 1.3 °C above the 1850–1900 reconstruction mean (Table 3b).

Table 2 Calibration and verification statistics for new June–August (JJA) northern hemispheric temperature reconstruction

Dependent data	**NH10-JJA**		
Independent data	CER		
Calibration period	1921–1965	1966–2010	1921–2010
Verification period	1966–2010	1921–1965	
R^2	0.429 (0.0020)	0.629 (< 0.0001)	0.585 (< 0.0001)
r^2	0.629 (< 0.0001)	0.429 (0.0020)	
RE	0.680	0.205	
CE	0.590	0.103	

The Berkeley Earth instrumental land temperature data averaged over grid boxes extending the sampling sites plus/minus 10 degrees latitudinally and longitudinally (see Fig. 1) were explained over the 1921–2010 period using CER data. The full calibration period is divided into early (1921–1965) and late (1966–2010) subperiods for cross-validation. The coefficient of determination (R^2) is calculated over the calibration period and squared coefficient of correlation (r^2) with their p values included in the parenthesis, and the reduction of error (RE) and coefficient of efficiency (CE) statistics over the verification period

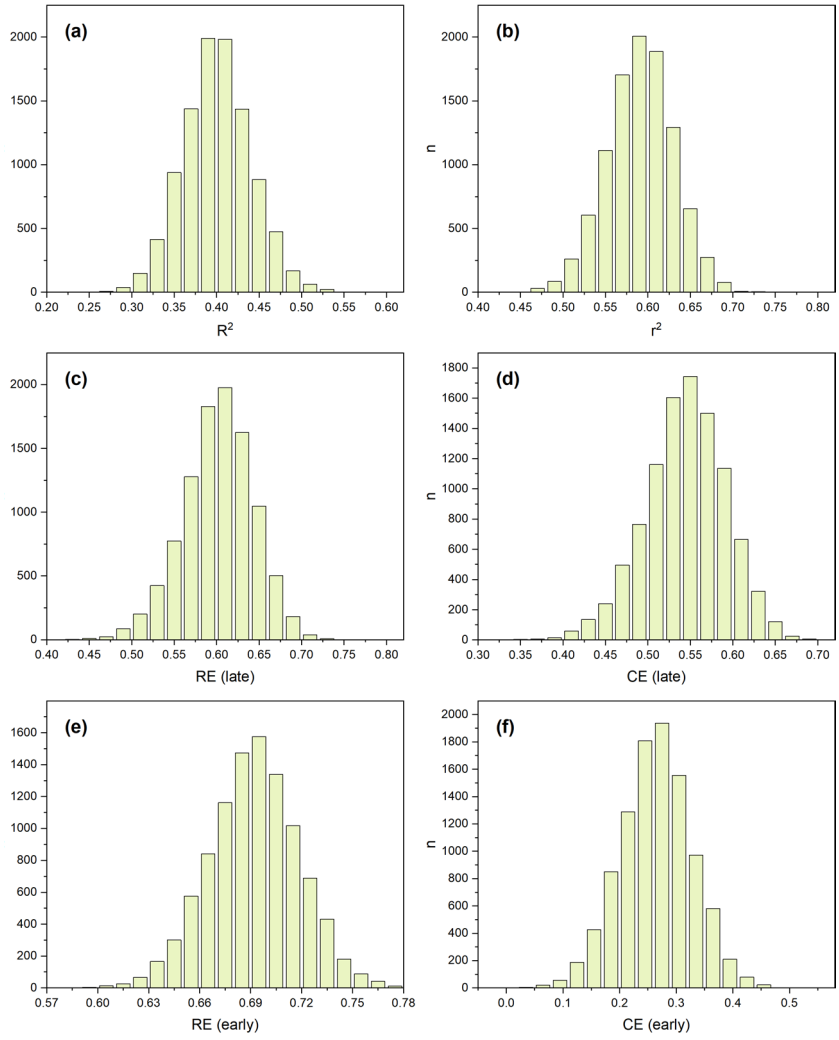

Fig. 3 Empirical probability density functions for the coefficient of determination (R^2) (**a**) and the squared coefficient of correlation (r^2) (**b**), the reduction of error (RE) (**c**, **e**), and coefficient of efficiency (CE) (**d**, **f**) statistics calculated over the early (1921–1965) and late (1966–2010) verification periods obtained from the bootstrapping of the individual ensemble members

Quantifying the upper and lower bounds of the 95% range for the reconstructed temperature data, an uncertainty of 0.90 to 1.63 °C for the JJA temperature of AD 246 was obtained (Fig. 4; Table 3b). Thus, comparison between the warmth in AD 246 and the warmest 21st century temperatures, especially those experienced in 2023 and 2024, shows that the recent warmth have exceeded the range of natural climate variability of the past 2000 years by 1.0 °C and 1.2 °C, respectively (Fig. 4), when considering the uncertainty. Similar estimates were found for the mean of the past ten summers (2016–2025) that appeared 1.3 °C higher than the mean of the ten warmest preindustrial summers.

The warmest and coldest reconstructed summers in AD 246 and AD 536 were, respectively, 1.5 °C and 5.5 °C colder than the 2024 warmth. Thus, the range of preindustrial temperature variability was 4.0 °C. Moreover, comparing the means of ten warmest and ten coldest preindustrial summers resulted in temperature difference of 3.2 °C. With these regards, the results indicated an occurrence of exceptionally warm summers

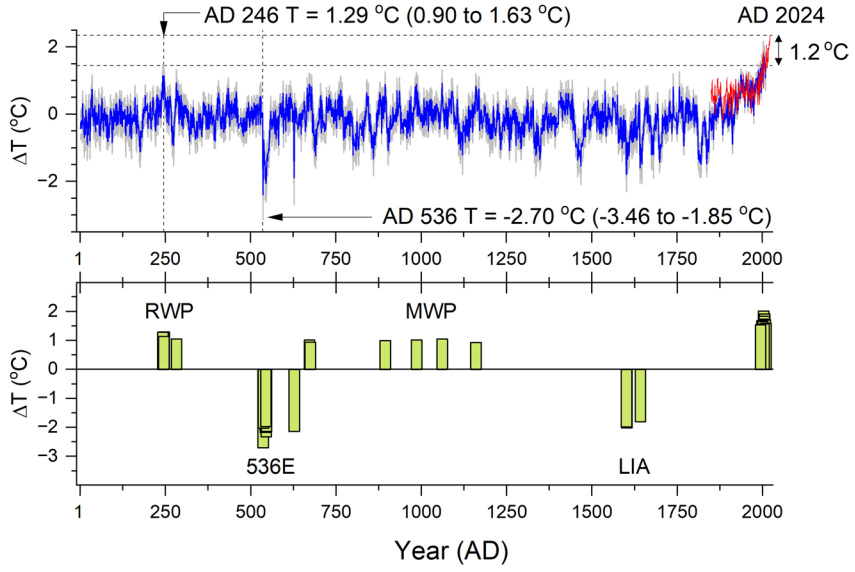

Fig. 4 New summer (June through August) temperature reconstruction (blue line) with bootstrapped 95% confidence interval (grey lines) and JJA instrumental land temperature NH10-JJA record. Vertical dashed lines display the warmest (246 CE) and coldest (536 CE) preindustrial summers, shown with the reconstructed temperatures (T) with 95% confidence interval for the two events. Horizontal dashed lines display the range of ~ 1.2 °C by which the summer 2024 warmth exceeded the natural climate variability considering the uncertainty (**a**). The warmest and coldest reconstructed temperature events plotted on a time axis (see Table 3 for numerical values) revel a pattern of long-term climatic swings through the Roman Warm Period (RWP), AD 536 event/540s (536E), Mediaeval Warm Period (MWP) and Little Ice Age (LIA) (**b**). Temperatures (ΔT) are shown relative to the preindustrial 1850–1900 reconstruction mean. See Table S1 for annual temperature values

during the third century AD (between AD 242 and AD 282) and a cluster of extremely cold summers in the sixth century AD (between AD 536 and AD 546). The sixth century AD climatic event was further demonstrated by a spell of years from AD 536 to 558 when temperatures remained below the preindustrial 1850–1900 reconstruction mean (Fig. 5b).

Focussing on the most extreme events, even a higher difference, 5.5 °C (4.7 °C considering the uncertainty), was found between the summers AD 2024 and AD 536. Clearly, the 21st century warm events have widened the range of Northern Hemisphere summer temperature variability by 1.5 °C.

3 Discussion

3.1 Instrumental and proxy data

CER data correlated well with Northern Hemisphere extra-tropical summer temperatures but did not verify successfully against the similarly represented instrumental records. Instead, CER data verified successfully when compared to temperature grid boxes around the tree-ring sites (Fig. 2). This issue has several ramifications to climate change research and climatic studies based on proxy data. Importantly, the results highlight the irreplaceable value of verification when new climate reconstructions are being built, especially when proxy data is utilized to place the recent climatic events in a long-term paleoclimatic context.

Essentially, verification of climatic reconstructions should be noted to have two principal goals. First, to assess the reliability of particular statistical model and its coefficients and, second, to express a universal property of that model so that it could be assumed

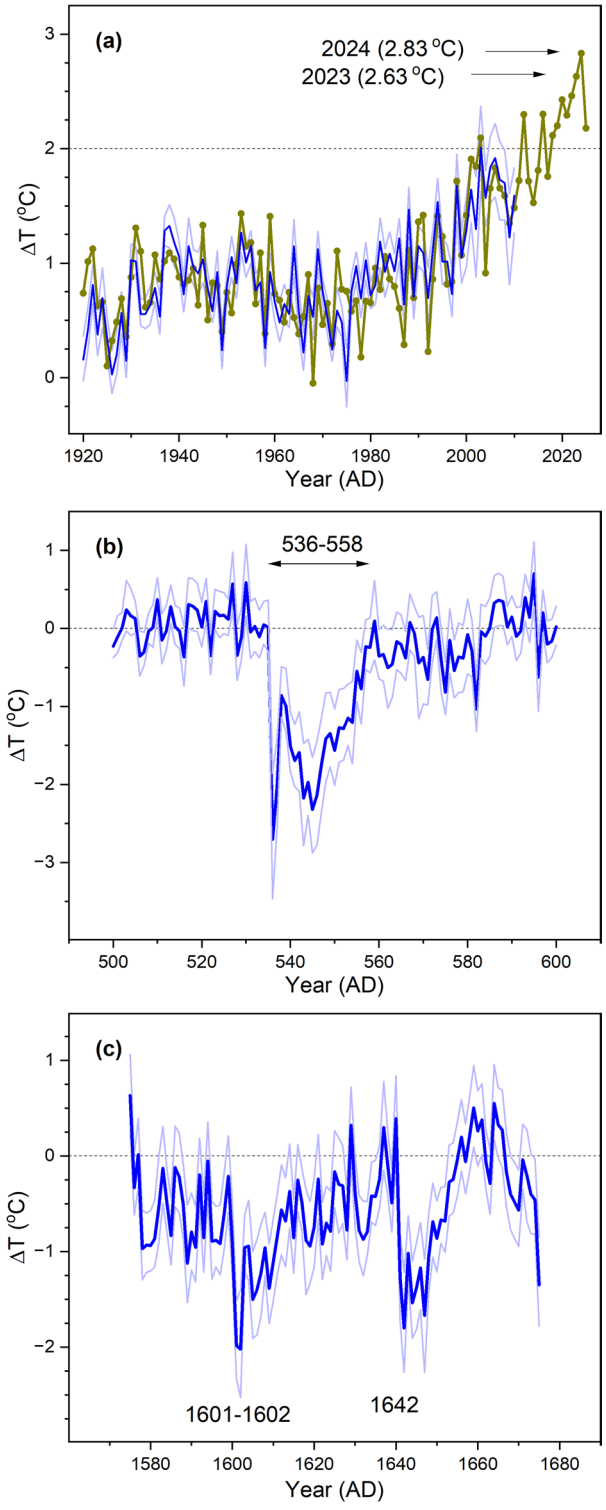

Fig. 5 Reconstructed summer (June through August) temperature variability (blue line) with bootstrapped 95% confidence interval (light blue), shown here since AD 1921 (**a**), for AD 500–600 period (**b**) and AD 1575–1675 period (**c**). The uppermost plot (**a**) shows also the instrumental NH10-JJA record (green). Temperatures are shown relative to the preindustrial 1850–1900 reconstruction mean

Table 3 The years with the most extreme temperature events

	Year (AD)	ΔT (°C)	L95 (°C)	U95 (°C)
(a)	2003	2.007	1.628	2.372
	2006	1.918	1.578	2.218
	2005	1.838	1.523	2.107
	2007	1.728	1.376	2.059
	2008	1.699	1.376	1.987
	1998	1.673	1.369	1.951
	2001	1.642	1.355	1.934
	2010	1.589	1.261	1.831
	2004	1.570	1.327	1.807
	1994	1.535	1.305	1.739
(b)	246	1.289	0.896	1.627
	242	1.285	0.901	1.635
	245	1.138	0.780	1.462
	282	1.047	0.579	1.492
	1061	1.041	0.631	1.469
	986	1.014	0.625	1.395
	672	1.009	0.639	1.374
	894	0.992	0.543	1.415
	674	0.941	0.552	1.329
	1160	0.931	0.508	1.347
(c)	536	-2.704	-3.463	-1.854
	545	-2.322	-2.879	-1.652
	543	-2.176	-2.784	-1.475
	546	-2.139	-2.777	-1.446
	627	-2.137	-2.931	-1.370
	537	-2.033	-2.559	-1.412
	1602	-2.022	-2.527	-1.406
	1601	-1.984	-2.336	-1.514
	544	-1.971	-2.396	-1.422
	1642	-1.801	-2.265	-1.219

The warmest reconstructed temperatures (a) and those reconstructed over the preindustrial period (AD 1-1900) (b), and the coldest temperatures over the full reconstruction period (AD 1-2025), described by temperature deviation (ΔT) from the preindustrial 1850–1900 reconstruction mean, and the lower (L95) and upper (U95) bounds of the 95% range around the reconstructed temperature

to apply over all periods of time [27, 34]. Recently, no verification was carried out when CER data based on which the Northern Hemisphere extra-tropical land temperatures (referred to here as NH-JJA) were reconstructed [18]. Had that analysis included verification statistics, they would have informed that the scaling of CER data against NH-JJA record is violated. Of note, a justification for skipping this analytical step was that verification had been previously [21] reported for various gridded CER-based temperature products [18]. Even so, such data exercises refer only to the second goal of verification, with no information about the validity of the particular statistical model used to transform proxy data into climatic estimates. In keeping with this view, any bias present in the training dataset may be unintentionally incorporated in the reconstruction [35]. This is critically important in the context of the present study since the comparisons between the past and 21st century warm events depend on precisely estimated temperature scale. Shortly, verification of climatic reconstructions is a routine procedure [28–29, 34] in testing the credibility of reconstruction models and it is difficult to imagine any meaningful norm to disregard this critical step of producing paleoclimate reconstructions from proxy data.

The upward temperature trend recorded here for NH10-JJA record especially since the 1990s could be viewed in the context of the Arctic amplification i.e. the warming of the Arctic region over the recent decades, relative to lower latitudes [36–38]. According to Rantanen et al. [39], the Arctic region (by which they referred to as 66.5°–90°N i.e. Arctic Circle poleward) has been warming nearly four times faster than the globe since 1979. The same authors compared the Arctic amplification ratios from observations and climate models and found that the four-fold warming ratio they documented over 1979–2021 was an extremely rare occasion in the climate model simulations [39]. Comparing several types of proxy data, Miller et al. [40] evaluated the occurrence and magnitude of Arctic amplifications under climate states both warmer and colder than present over the past three million years. According to their estimates, the Arctic temperature change has consistently exceeded the Northern Hemisphere average by a factor of 3–4 [40]. Their findings have at least two ramifications relevant to the present study. First, as Miller et al. [40] suggested, their results mean that the Arctic warming will continue to exceed the warming of global average temperature over the 21st century. Second, it could also be indicated that the climatic events recorded here using proxy data over the past two thousand years possibly reflect the same phenomenon, the Arctic amplification. The presented results of verification, indicating that CER data may not be representative of the full extra-tropical Northern Hemisphere, point to issues relevant also to this discussion. Shortly, proxy data should not be used to infer past or recent temperature variations beyond the grid boxes identified as their valid counterpart. Here, NH10-JJA record served as an element of Northern Hemisphere temperature history mirrored by CER data. This meant that many southern regions of the extra-tropical Old World remained beyond the reach of the new AD 1-2025 temperature record (see Fig. 1).

Yet another issue the verification statistics revealed was the disparity between the instrumental and CER data over the two first decades of the 20th century. Calculated over the 1901–1920 period, the offset between the reconstruction and NH10-JJA was 0.6 °C (instrumental temperatures warmer than proxy ones, see Fig. 2f). Parallel, but slightly smaller offsets, 0.4 °C and 0.5 °C, could be similarly calculated for the 1850–1900 and 1850–1920 periods, respectively (not shown). These estimates are of a similar magnitude to previous assessments between the different hemispheric temperature products and their tree ring reconstructions. A warm bias in the extra-tropical Northern Hemisphere instrumental summer temperatures was previously demonstrated prior to ~ 1900 [15]. Later assessments [41] demonstrated tree-ring based summer temperature reconstructions to show on average 0.39 °C colder conditions from 1851 to 1900 with a range of 0.19°–0.55 °C among six records their worked with, in comparison to the extra-tropical Northern Hemisphere instrumental land temperatures. The Berkeley Earth temperature dataset [5], used also in the present study, was previously found to show the smallest offset between instrumental and tree-ring data, which was assumed to indicate that additional stations included in this product could have led to cooler 19th century temperatures [41]. The largest exposure biases are indeed expected in mean temperatures and in summer [23]. Apart from problems in instrumental data, another plausible factor behind the offset may relate to inertia of biological processes affecting the proxy data such as tree-ring records [15]. Hypothetically, a combination of such inertia and coldness of the 19th century could have led to a progressively weak growth phase, and thus proxy-based estimations that fall below the actual level of prevailing air temperatures

over the 1850–1900 period. Even so, the existing literature seems to put more weight on the problems that characterize the instrumental observations [41]. What is certain is the increase of uncertainties in both instrumental and tree-ring data when the records are extended back in time, to the 19th century (not to mention earlier times), when the instrumentation of meteorological stations [23, 30] and conditions to tree growth [42, 43] have both been much different to present day.

Scaling CER data over the full 20th century, without excluding the problematic early decades of the 20th century, resulted in verification statistics that did not indicate skill in the reconstruction (Fig. 2a–d). In this study, this bias was avoided by calibrating CER data over the 1921–2010 period for which interval the scaling CER to NH10-JJA record resulted in invariably positive verification statistics (Table 2; Fig. 3). Overall, it should be borne in mind that shaping the size of the training set cannot be done without information from independent sources. It should, nonetheless, be carried out instead of processing noisy data as otherwise the proxy-based estimates are invariably biased [35, 44]. Specific to instrumental data with expose bias, calibrating proxy data against such data will unavoidably yield to deflated proxy-based temperature variance. This is logical since the exposure bias is expected to diminish the variance of instrumental data in relation to proxy values (Fig. 2f). Excluding the early decades of the 20th century, over which period the exposure bias has been independently described [22, 23], on the other hand, resulted in precisely estimated temperature scale, at least insofar as could be indicated from the verification statistics. Collectively, these considerations demonstrate the ways the procedures used here to build the new reconstruction are expected to benefit the proxy-based estimations of preindustrial climate variability and, as a result, create a more reliable long-term context for 21st century warming.

3.2 New temperature reconstruction

Magnitude of the current warming exceeded the range of past warm events that are inferred from CER data (Figs. 4 and 5a). While the highest values recorded during the 21st century were based on instrumental data, the list of the warmest reconstructed events was likewise shaped by summers of the past 30 years (Table 3a). Placing these estimates into a long-term context provides ways CER data contributes to understanding the state of our planet. That being said the NH10-JJA reconstruction represents only one out of four seasons and is geographically limited to regions around the tree-ring sites. It is also notable that despite the reconstruction was supported by positive verification statistics (Fig. 2c), there were years even over the 1921–2010 period during which the NH10-JJA and CER data did not fully agree (Fig. 2f). This means that similar instances may have occurred in the past and, accordingly, the reconstructed events may not cover the full spectrum of the 2000-year temperature history. Alternatively, extent of some of the past events may be overestimated. The extent to which instrumental data may or may not represent the weather over the sites of tree growth was addressed in the previous section. It should also be born in mind that there are several ways to transform proxy data values into temperature estimates, but none of the methods are wholly satisfactory [45]. To this discussion can be added a cautionary note made by Briffa et al. [46] that though temperature may strongly affect tree growth, trees are still not thermometers. Instead, the temperature limitation appears as part of a complex ecology involving

biochemical processes that are also influenced by factors other than climate. It follows that tree-ring data can only be climatically interpreted under simplifying assumptions [46].

Moreover, there are several ways to compare the current warming with preindustrial temperatures. The choice of AD 1850–1900 period as a preindustrial baseline probably originates from Allen et al. [14] and has been intensively used thereafter. Comparing the recent temperatures with the preindustrial 1850–1900 reconstruction mean level avoids the expected biases in early temperature observations [18]. In the present study, this approach demonstrates recent summer temperatures to exceed the foregoing level by well more than 2.0 °C (Figs. 4 and 5a), this magnitude representing change between a cold Holocene phase [47] and the current warming. A more conservative estimate makes use of CER data over the past two thousand years. Also considering the uncertainty around the reconstructed values, the summers 2023 and 2024 show warming that appears to have exceeded the range of natural climate variability by ~ 1.0 °C and 1.2 °C. These values are approx. three-folded compared to previous estimates relying on a very similar comparison but using summer 2023 observations [18, 19], additional difference being a result of elaborated calibration of proxy-data in the present study (i.e. the use of NH10-JJA instead of NH-JJA, as detailed above).

The highest temperatures could also be compared with the events of coldest years (Table 3c). According to CER data, the strongest cold phase occurred during the mid-sixth century AD when temperatures dropped in AD 536 (Fig. 4; Table 3c) and remained below the preindustrial 1850–1900 reconstruction mean until the end of AD 550s (Fig. 5b). These perturbations demonstrate the 'AD 536/540s event' during which the drop in summer temperatures have been recorded in several tree-ring studies [18, 21, 48–55]. The deteriorated conditions were driven by volcanic dust veil [56–58] from large explosive eruptions in (AD 535/536 and AD 539/540 [59] that strongly reduced the amount of incoming solar radiation in the course of several post-eruption years [60]. Compared to previous notes [18, 21], it is notable that the post-eruption event did not seem to last longer than a few decades, in agreement with findings from several other collections of proxy data [59, 61, 62]. Another set of cold events occurred during the 17th century AD (Table 3c; Figs. 4b and 5c) that belongs to the period between AD 1570 and 1900 when extra-tropic Northern Hemisphere summer temperatures fell markedly below the late 20th century level [63], which overlaps with the Little Ice Age from about AD 1250 to 1860 [64]. Similar to the AD 536/540s event, the 17th century cold events (Table 3c) have been previously associated with volcanic forcing [65] hence representing the characteristics of the natural temperature variability opposing the current warming, which has now extended the full range of natural summer temperature variability in the study region from 4.0 °C to 5.5 °C. Alternatively, the current warming may be compared to its possible late Holocene counterparts such as the 'Mediaeval Warm Period' [66, 67] (alternatively, the 'Medieval Climate Anomaly' [68]). With these regards, it has been thought that the importance of characterising the climate in medieval times (AD ~ 800–1250) is to develop greater insights into the range of past climate variability in comparison with the modern instrumental period [69, 70]. It is as well of value to address the question, whether the ongoing warming is unusual in such a late Holocene context [71–73]. Strong warm events coeval to the Mediaeval Warm Period were reconstructed here between AD 894 and 1160 (Table 3b). Even so, the strength of the warmest Mediaeval

temperature events appeared ~ 1.0 °C and ~ 1.8 °C lower than those recently reconstructed (Table 3a) and instrumentally recorded (Fig. 5a), respectively. Moreover, these preindustrial events are spread over an interval of two and half centuries (Fig. 4), in comparison to the recently observed warm summers that cluster within the past 30 years. This, again, demonstrates the increased likelihood of extremely warm individual summers evoked by the recent upward trend in summer temperatures [20].

Even warmer preindustrial events were, however, recorded during the AD 240s and 280s (Fig. 4; Table 3b). The AD 246 summer warmth in CER data was previously related to the 'Roman Warm Period', as were the warm events recorded in Fennoscandian tree-ring data between AD 21 and 50 [18, 74]. The climatic conditions characterising the Roman times were already noted by Lamb [67, 75], by which he referred a tendency towards warmth in Europe until about AD 400, as indicated by various kinds of documentary and proxy data. More recently, Harper and McCormick [76] supported calling the period 200 BC to AD 150 the 'Roman Climate Optimum', as this interval would more topically overlap the phase of warm climate in the circum-Mediterranean territories. In comparison, CER data represent temperature variations over much wider spatial domains (Fig. 1), implying that the warm events recorded here for the early centuries of the first millennium are not limited to the Mediterranean or European territories. Clearly, the Roman Warm Period (including the third century AD warmth) warrants further high-resolution investigations in much widened geographical contexts. What should be born in mind is that such evaluations and comparisons between the past and recent warm events need to contemplate the Milankovitch forcing and thus the decrease in summer insolation evident for CER sites' latitudes over the past millennia [77–79]. A concomitant cooling with a long-term trend of 0.13 °C (± 0.01 °C) per 1000 years was recently recorded in tree-ring data from Fennoscandia, in agreement with a circumpolar dataset including various types of sedimentary proxy records sensitive to summer temperature variations [80]. On these grounds, a change in temperature background level corresponding to a quarter of a centigrade could be expected from Roman to recent times, which further underlines the extent of the 20th and 21st century warm events in the context of the past millennia.

Supplementary Information

The online version contains supplementary material available at https://doi.org/10.1007/s44288-026-00523-4.

Supplementary Material 1.

Acknowledgements
Four anonymous reviewers provided a review of the manuscript, for which I am grateful.

Author contributions
SH designed the study, analysed the data, wrote the manuscript and prepared the tables and figures.

Funding
This study was supported by the Research Council of Finland (339788, 355268).

Data availability
CER and NH-JJA records are available at https://doi.org/10.17605/OSF.IO/MDUVK and the data for NHS-JJA, NH10-JJA and NH20-JJA records are available at https://berkeleyearth.org/data/.

Declarations

Ethics approval and consent to participate
Not applicable.

Consent for publication
Not applicable.

Competing interests
The authors declare no competing interests.

Received: 10 October 2025 / Accepted: 10 April 2026
Published online: 18 April 2026

References

1. Jones P, Wigley T, Wright P. Global temperature variations between 1861 and 1984. Nature. 1986;322:430–4. https://doi.org/10.1038/322430a0.
2. Jones PD, New M, Parker DE, et al. Surface air temperature and its changes over the past 150 years. Rev Geophys. 1999;37:173–99. https://doi.org/10.1029/1999RG900002.
3. Peterson TC, Vose R. An overview of the global historical climatology network temperature database. Bull Am Meteorol Soc. 1997;78:2837–49. https://doi.org/10.1175/1520-0477(1997)078%3C2837:AOOTGH%3E2.0.CO;2.
4. Brohan P, Kennedy JJ, Harris I, et al. Uncertainty estimates in regional and global observed temperature changes: A new data set from 1850. J Geophysiscal Res. 2006;111. https://doi.org/10.1029/2005JD006548.
5. Rohde R, Muller R, Jacobsen R et al. 2013. A new estimate of the average Earth surface land temperature spanning 1753 to 2011. Geoinformatics & Geostatistics: An Overview 1. https://doi.org/10.4172/gigs.1000103
6. Xu W, Li Q, Jones P, et al. A new integrated and homogenized global monthly land surface air temperature dataset for the period since 1900. Clim Dyn. 2018;50:2513–36. https://doi.org/10.1007/s00382-017-3755-1.
7. Taylor M, Osborn TJ, Cowtan K, et al. GloSAT LATsdb: A Global Compilation of Land Air Temperature Station Records With Updated Climatological Normals From Local Expectation Kriging. Geosci Data J. 2025;12. https://doi.org/10.1002/gdj3.70024.
8. Osborn TJ, Jones PD, Lister DH, et al. Land surface air temperature variations across the globe updated to 2019: the CRUTEM5 dataset. J Phys Res. 2021;126. https://doi.org/10.1029/2019JD032352.
9. Li Q, Sun W, Yun X, et al. An updated evaluation of the global mean land surface air temperature and surface temperature trends based on CLSAT and CMST. Clim Dyn. 2021;56:635–50. https://doi.org/10.1007/s00382-020-05502-0.
10. Samset BH, Lund MT, Fuglestvedt JS, et al. 2023 temperatures reflect steady global warming and internal sea surface temperature variability. Commun Earth Environ. 2024;5. https://doi.org/10.1038/s43247-024-01637-8.
11. Cheng L, Abraham J, Trenberth KE, et al. Record High Temperatures in the Ocean in 2024. Adv Atmos Sci. 2025;42:1092–109. https://doi.org/10.1007/s00376-025-4541-3.
12. Logan G, Ciavarella A, McCarthy M. An Attribution Study of the UK mean temperature in summer 2025. Met Office, Hadley Centre; 2025.
13. Samset BH, Zhou C, Fuglestvedt JS, et al. Steady global surface warming from 1973 to 2022 but increased warming rate after 1990. Commun Earth Environ. 2023;4. https://doi.org/10.1038/s43247-023-01061-4.
14. Allen M, Dube OP, Solecki W, et al. Special Report: Global Warming of 1.5˚C. Intergovernmental Panel on Climate Change (IPCC); 2018.
15. Frank D, Büntgen U, Böhm R, et al. Warmer early instrumental measurements versus colder reconstructed temperatures: shooting at a moving target. Q Sci Rev. 2007;26:3298–310. https://doi.org/10.1016/j.quascirev.2007.08.002.
16. Bradley RS. Paleoclimatology: Reconstructing Climates of the Quaternary. Burlington, Harcourt-Academic Press; 1999.
17. McCulloch MT, Winter A, Sherman CE, et al. 300 years of sclerosponge thermometry shows global warming has exceeded 1.5°C. Nat Clim Change. 2024;14:171–7. https://doi.org/10.1038/s41558-023-01919-7.
18. Esper J, Torbenson M, Büntgen U. 2023 summer warmth unparalleled over the past 2,000 years. Nature. 2024;631:94–7. https://doi.org/10.1038/s41586-024-07512-y.
19. Esper J, Torbenson M, Büntgen U. Author Correction: 2023 summer warmth unparalleled over the past 2,000 years. Nature 2025;641:E11. https://doi.org/10.1038/s41586-025-09095-8
20. Rantanen M, Helama S, Räisänen J, et al. Summer 2024 in northern Fennoscandia was very likely the warmest in 2000 years. npj Clim Atmospheric Sci. 2025;8:1–11. https://doi.org/10.1038/s41612-025-01046-4.
21. Büntgen U, Allen K, Anchukaitis KJ, et al. The influence of decision-making on tree ring-based climate reconstructions. Nat Commun. 2021;12. https://doi.org/10.1038/s41467-021-23627-6.
22. Folland CK, Rayner NA, Brown SJ, et al. Global temperature change and its uncertainties since 1861. Geophys Res Lett. 2001;28:2621–4. https://doi.org/10.1029/2001GL012877.
23. Wallis EJ, Osborn TJ, Taylor M, et al. Quantifying exposure biases in early instrumental land surface air temperature observations. Int J Climatol. 2024;44:1611–35. https://doi.org/10.1002/joc.8401.
24. Briffa KR, Osborn TJ, Schweingruber FH, et al. Low-frequency temperature variations from a northern tree ring density network. J Phys Res. 2001;106:2929–41. https://doi.org/10.1029/2000JD900617.
25. Briffa KR, Osborn TJ, Schweingruber FH, et al. Tree-ring width and density data around the Northern Hemisphere: Part 1, local and regional climate signals. Holocene. 2002a;12:737–51. https://doi.org/10.1191/0959683602hl587rp.
26. Briffa KR, Osborn TJ, Schweingruber FH, et al. Tree-ring width and density data around the Northern Hemisphere: Part 2, spatio-temporal variability and associated climate patterns. Holocene. 2002b;12:759–89. https://doi.org/10.1191/0959683602hl588rp.
27. Gordon GA, Gray BM, Pilcher JR. Verification of dendroclimatic reconstructions. In: Hughes MK, Kelly PM, Pilcher JR, editors. et al. Climate from Tree Rings. Cambridge: Cambridge University Press; 1982. pp. 58–62.
28. Fritts HC. Tree rings and climate. New York: Academic; 1976.
29. Briffa KR, Jones PD, Pilcher JR, et al. Reconstructing summer temperatures in Northern Fennoscandinavia back to A.D. 1700 using tree-ring data from Scots pine. Arct Alp Res. 1988;20:385–94. https://doi.org/10.2307/1551336.
30. Naylor S. Thermometer screens and the geographies of uniformity in nineteenth-century meteorology. Notes Records. 2018;73:203–21. https://doi.org/10.1098/rsnr.2018.0037.

31. Macias-Fauria M, Grinsted A, Helama S, et al. Persistence matters: Estimation of the statistical significance of paleoclimatic reconstruction statistics from autocorrelated time series. Dendrochronologia. 2012;30:179–87. https://doi.org/10.1016/j.dendro.2011.08.003.
32. Ebisuzaki W. A method to estimate the statistical significance of a correlation when the data are serially correlated. J Clim. 1997;10:2147–53. https://doi.org/10.1175/1520-0442(1997)010%3C2147:AMTETS%3E2.0.CO;2.
33. Loader N, Young G, McCarroll D, et al. Quantifying uncertainty in isotope dendroclimatology. Holocene. 2013;23:1221–6. https://doi.org/10.1177/0959683613486945.
34. Fritts HC, Guiot, Gordon GA. Verification in Methods of Dendrochronology. In: Cook ER, Kairiukstis LA, editors. Methods of dendrochronology: applications in the environmental sciences. Dordrecht: Kluwer Academic; 1990. pp. 178–85.
35. Briffa KR, Osborn TJ, Schweingruber FH. Large-scale temperature inferences from tree rings: a review. Glob Planet Change. 2004;40:11–26. https://doi.org/10.1016/S0921-8181(03)00095-X.
36. Serreze MC, Francis JA. The Arctic Amplification Debate. Clim Change. 2006;76:241–64. https://doi.org/10.1007/s10584-005-9017-y.
37. Serreze MC, Barry RG. Processes and impacts of Arctic amplification: A research synthesis. Glob Planet Change. 2011;77:85–96. https://doi.org/10.1016/j.gloplacha.2011.03.004.
38. Previdi M, Smith KL, Polvani LM. Arctic amplification of climate change: a review of underlying mechanisms. Environ Res Lett. 2021;16. https://doi.org/10.1088/1748-9326/ac1c29.
39. Rantanen M, Karpechko AY, Lipponen A, et al. The Arctic has warmed nearly four times faster than the globe since 1979. Commun Earth Environ. 2022;3. https://doi.org/10.1038/s43247-022-00498-3.
40. Miller GF, Alley RB, Brigham-Grette J, et al. Arctic amplification: can the past constrain the future? Q Sci Rev. 2010;29:1779–90. https://doi.org/10.1016/j.quascirev.2010.02.008.
41. Schneider L, Konter O, Esper J, et al. Constraining the nineteenth-century temperature baseline for global warming. J Clim. 2023;36:6261–72. https://doi.org/10.1175/JCLI-D-22-0806.1.
42. Hustich I. Climatic Fluctuations and Vegetation Growth in Northern Finland During 1890–1939. Nature. 1947;160:478–9. https://doi.org/10.1038/160478a0.
43. Nicolussi K, Bortenschlager S, Körner C. Increase in tree-ring width in subalpine *Pinus cembra* from the central Alps that may be CO_2-related. Trees. 1995;9:181–9. https://doi.org/10.1007/BF00195270.
44. Cook ER, Palmer JG, Cook BI, et al. A multi-millennial palaeoclimatic resource from *Lagarostrobos colensoi* tree-rings at Oroko Swamp, New Zealand. Glob Planet Change. 2002;33:209–20. https://doi.org/10.1016/S0921-8181(02)00078-4.
45. Christiansen B, Ljungqvist FC. Challenges and perspectives for large-scale temperature reconstructions of the past two millennia. Rev Geophys. 2017;55:40–96. https://doi.org/10.1002/2016RG000521.
46. Briffa KR, Jones PD, Schweingruber FH, et al. Tree-ring variables as proxy-climate indicators: Problems with low-frequency signals. In: Jones PD, Bradley RS, Jouzel J, editors. Climatic Variations and Forcing Mechanisms of the Last 2000 Years. Berlin: Springer-; 1996. pp. 9–41. https://doi.org/10.1007/978-3-642-61113-1_2.
47. Lüning S, Vahrenholt F. Paleoclimatological context and reference level of the 2°C and 1.5°C Paris agreement long-term temperature limits. Front Earth Sci. 2017;5:1–7. https://doi.org/10.3389/feart.2017.00104.
48. Briffa K, Bartholin T, Eckstein D, et al. A 1,400-year tree-ring record of summer temperatures in Fennoscandia. Nature. 1990;346:434–9. https://doi.org/10.1038/346434a0.
49. Scuderi LA. Tree-Ring Evidence for Climatically Effective Volcanic Eruptions. Quatern Res. 1990;34:67–85. https://doi.org/10.1016/0033-5894(90)90073-T.
50. Baillie MGL. Dendrochronology raises questions about the nature of the AD 536 dust-veil event. Holocene. 1994;4:212–7. https://doi.org/10.1177/09596836940040021.
51. Naurzbaev MM, Vaganov EA, Sidorova OV, et al. Summer temperatures in eastern Taimyr inferred from a 2427-year late-Holocene tree-ring chronology and earlier floating series. Holocene. 2002;12(6):727–36. https://doi.org/10.1191/0959683602hl586rp.
52. Salzer MW, Hughes MK. Bristlecone pine tree rings and volcanic eruptions over the last 5000 year. Quatern Res. 2007;67:57–68. https://doi.org/10.1016/j.yqres.2006.07.004.
53. Helama S, Holopainen J, Macias-Fauria M, et al. A chronology of climatic downturns through the mid- and late-Holocene: Tracing the distant effects of explosive eruptions from palaeoclimatic and historical evidence in northern Europe. Polar Res. 2013;32. https://doi.org/10.3402/polar.v32i0.15866.
54. Jones PD, Melvin TM, Harpham C, et al. Cool North European summers and possible links to explosive volcanic eruptions. J Phys Res. 2013;118:6259–65. https://doi.org/10.1002/jgrd.50513.
55. Stoffel M, Khodri M, Corona C, et al. Estimates of volcanic-induced cooling in the Northern Hemisphere over the past 1,500 years. Nat Geosci. 2015;8:784–8. https://doi.org/10.1038/ngeo2526.
56. Stothers RB, Rampino MR. Volcanic eruptions in the Mediterranean before A.D. 630 from written and archaeological sources. J Phys Res. 1983;88:6357–71. https://doi.org/10.1029/JB088iB08p06357.
57. Stothers R. Mystery cloud of AD 536. Nature. 1984;307:344–5. https://doi.org/10.1038/307344a0.
58. Arjava A. The Mystery Cloud of 536 CE in the Mediterranean sources. Dumbart Oaks Papers. 2005;59:73–94.
59. Sigl M, Winstrup M, McConnell JR, et al. Timing and climate forcing of volcanic eruptions for the past 2,500 years. Nature. 2015;523:543–9. https://doi.org/10.1038/nature14565.
60. Helama S, Arppe L, Uusitalo J, et al. Volcanic dust veils from sixth century tree-ring isotopes linked to reduced irradiance, primary production and human health. Sci Rep. 2018;8. https://doi.org/10.1038/s41598-018-19760-w.
61. Larsen LB, Vinther BM, Briffa KR, et al. New ice core evidence for a volcanic cause of the A.D. 536 dust veil. Geophys Res Lett. 2008;35. https://doi.org/10.1029/2007GL032450.
62. Helama S, Jones PD, Briffa KR. Limited Late Antique cooling. Nat Geosci. 2017;10:242–3. https://doi.org/10.1038/ngeo2926.
63. Matthews JA, Briffa KR. The 'Little Ice Age': re-evaluation of an evolving concept. Geogr Ann. 2005;87A:17–36. https://doi.org/10.1111/j.0435-3676.2005.00242.x.
64. Wanner H, Pfister C, Neukom R. The variable European Little Ice Age. Q Sci Rev. 2022;287:1–13. https://doi.org/10.1016/j.quascirev.2022.107531.
65. Briffa KR, Jones PD, Schweingruber FH, et al. Influence of volcanic eruptions on Northern Hemisphere summer temperature over the past 600 years. Nature. 1998;393:450–5. https://doi.org/10.1038/30943.

66. Lamb HH. The early medieval warm epoch and its sequel. Palaeogeography, Palaeoclimatology, Palaeoecology. 1965;1:13–37.
67. Lamb HH. Climate History and the Modern World. 2nd Edition. Routledge, New York. 1995.
68. Stine S. Extreme and persistent drought in California and Patagonia during medieval time. Nature. 1994;369:546–9. https://doi.org/10.1038/369546a0.
69. Ljungqvist FC, Krusic PJ, Brattström G, et al. Northern Hemisphere temperature patterns in the last 12 centuries. Clim Past. 2012;8:227–49. https://doi.org/10.5194/cp-8-227-2012.
70. Ljungqvist FC, Zhang Q, Brattström G, et al. Centennial-Scale Temperature Change in Last Millennium Simulations and Proxy-Based Reconstructions. J Clim. 2019;32:2441–82. https://doi.org/10.1175/JCLI-D-18-0525.1.
71. Mann ME, Zhang Z, Turherford S, et al. Global Signatures and Dynamical Origins of the Little Ice Age and Medieval Climate Anomaly. Science. 2009;326:1256–60. https://doi.org/10.1126/science.1177303.
72. Björklund J, Seftigen K, Stoffel M, et al. Fennoscandian tree-ring anatomy shows a warmer modern than medieval climate. Nature. 2023;620:97–103. https://doi.org/10.1038/s41586-023-06176-4.
73. Helama S. Low-frequency patterns in Late-Holocene tree-ring records from northern Fennoscandia. Holocene. 2025;35:654–60. https://doi.org/10.1177/09596836251320323.
74. Esper J, Frank DC, Timonen M, et al. Orbital forcing of tree-ring data. Nat Clim Change. 2012;2:862–6. https://doi.org/10.1038/nclimate1589.
75. Lamb HH. Our changing climate, past and present. Weather. 1959;14:299–318. https://doi.org/10.1002/j.1477-8696.1959.tb00533.x.
76. Harper K, McCormick M. Reconstructing the Roman Climate. In: Scheidel W, editor. The Science of Roman History Biology, Climate, and the Future of the Past. Princeton: Princeton University Press; 2018. pp. 11–52.
77. Berger A. Long-term variations of caloric insolation resulting from the earth's orbital elements. Quatern Res. 1978;9:139–67. https://doi.org/10.1016/0033-5894(78)90064-9.
78. Berger A. Milankovitch theory and climate. Rev Geophys. 1988;26:624–57. https://doi.org/10.1029/RG026i004p00624.
79. Berger A, Loutre MF. Insolation values for the climate of the last 10 million years. Q Sci Rev. 1991;10:297–317. https://doi.org/10.1016/0277-3791(91)90033-Q.
80. Helama S, Herva H, Arppe L, et al. Disentangling the evidence of Milankovitch forcing from tree-ring and sedimentary records. Front Earth Sci. 2022;10. https://doi.org/10.3389/feart.2022.871641.

Publisher's Note